第38卷第10期 2022年10月
无 机 化 学 学 报 CHINESE JOURNAL OF INORGANIC CHEMISTRY
Vol.38 No.10 2083-2090

镉基杂化晶体的介电相变和蓝白光致发光双重特性

吴 婷 丁 坤 伦蒙蒙 张 铁 张 毅* 付大伟*
(东南大学,分子铁电科学与应用江苏省重点实验室,有序物质科学研究中心,南京 211189)

摘要: 通过采用容易无序的胺,我们合成了2种有机无机杂化晶体,分别为基于bempy(bempy=1-甲基-1-溴乙基吡咯烷阳离子)的溴盐化合物(bempy)Br (**1**)和镉基溴化物$(bempy)_2CdBr_4$ (**2**),并对其结构相变、介电相变和蓝白荧光进行了详细的表征分析。化合物**1**在测试温度范围内未观察到可逆相变,化合物**2**为高温介电相变,介电和差示扫描量热法测试表征其相变温度为357 K。同时,化合物**1**和**2**均具备蓝白光致发光特性,荧光测试表明,化合物**1**和**2**分别在538 nm和547、750 nm处存在发射峰。化合物**2**具备介电相变和蓝白光致发光的双重特性。

关键词: 相变; 光致发光; 介电; 有机无机杂化
中图分类号: O614.24+2 **文献标识码:** A **文章编号:** 1001-4861(2022)10-2083-08
DOI: 10.11862/CJIC.2022.200

Dual Functions of Phase-Transition Dielectric and Blue-White Photoluminescence in a Hybrid Crystal $(bempy)_2CdBr_4$

WU Ting DING Kun LUN Meng-Meng ZHANG Tie ZHANG Yi* FU Da-Wei*
(*Ordered Matter Science Research Center, Jiangsu Key Laboratory for Science and Applications of Molecular Ferroelectrics, Southeast University, Nanjing* 211189, *China*)

Abstract: We have successfully synthesized two organic-inorganic hybrid crystals, which are (bempy)Br (**1**) and $(bempy)_2CdBr_4$ (**2**), based on bempy (bempy=1-bromoethyl-1-methylpyrrolidinium) by employing easily disordered amines. Structural phase transitions analysis, dielectric phase transition measurements, and blue-white fluorescence spectroscopy measurements were performed on them. It is notable that, no reversible phase transition was observed in compound **1**, and compound **2** exhibited high-temperature dielectric phase transition anomalies at around 357 K by differential scanning calorimetry and dielectric measurements. Both compounds showed blue-white photoluminescence with one emission peak at 538 nm for compound **1** and two emission peaks at 547 and 750 nm for compound **2**. Significantly, compound **2** possesses dual functions of dielectric phase transition and blue-white photoluminescence. CCDC: 2155028, **1**; 2155029, **2**.

Keywords: phase transition; photoluminescence; dielectric; organic-inorganic hybrid

Multifunctional materials with both photoluminescence and phase transition properties, as a new type of photoelectric materials, possess great potential applications in solar cells, sensors, optoelectronic components, *etc*[1-5]. Organic-inorganic hybrid metal halides have been studied as candidates for light-emitting materials due to their structural tunability, superior stability, easy preparation, *etc*[6-13]. Meanwhile, much attempt has been made to achieve bistable dielectric switch materials through organic-inorganic hybridization[14-20]. It is

收稿日期:2022-04-16。收修改稿日期:2022-08-07。
国家自然科学基金(No.21673038)资助。
*通信联系人。E-mail:dawei@seu.edu.cn,yizhang1980@seu.edu.cn

worthwhile to combine reversible phase transitions and luminescence within organic-inorganic hybrids, which will both realize the dielectric switch and achieve tunable luminescence properties[21-23]. The phase transitions of crystalline materials may be related to the internal structure of organic cations for their diversity and tunability[24-25]. A large amount of organic-inorganic hybrids, such as (pyrrolidinium)$MnCl_3$[26], (*R*)- and (*S*)-3-(fluoropyrrolidinium)$MnCl_3$[27], and (3-pyrrolinium)$MnCl_3$[28], have been proved to be excellent perovskite-type phase-transition dielectrics and ferroelectrics with photoluminescence. More importantly, it was considered to be effective to modify organic cations by introducing halogen, which may consciously tune the dielectric properties of materials[29-34]. The course of designing and synthesizing new phase-transition materials by introducing different halogens would open up wireless possibilities.

Therefore, the organic-inorganic hybrid metal halides, as significant functional carriers, offer possibilities for materials with both luminescent and electrical stimuli-responsive properties[35]. On the one hand, phase transitions caused by the motion of organic cations would be implemented via tuning organic cation frameworks[5,36-39]. On the other hand, it is meaningful to select different inorganic coordination metal ions and coordination modes to design ideal photoluminescence properties[40-42]. Low-electronegativity transition metals have usually been reported to exhibit remarkable photoluminescence properties owing to their unfilled valence *d* orbitals[43], such as manganese-based hybrid materials, based on various metal-ion coordination geometry, often emit different colors with green, red, *etc*[44-46]. Polynuclear d^{10} metal spatial cadmium has also attracted much attention for its photoluminescence, optical, and electrical properties, exhibiting blue or blue-white emissions at different excitation wavelengths[47]. As we all know, white light emission shows great significance, and single-component white light-emitting materials would become promising candidates for the replacement of traditional solid-state lighting[7]. It is fortunate that metal ion with d^{10} configuration, Cd^{2+}, was able to function as a luminescent center to obtain highly efficient broadband white-light emission. Previous studies on Cd halides with white-light emission and dielectric phase change, however, have rarely been reported[48].

Inspired by the regulation of organic cation and the introduction of d^{10} configuration metal ion Cd^{2+}, we have successfully synthesized two photoelectric materials, (bempy)Br (**1**) and $(bempy)_2CdBr_4$ (**2**) (bempy=1-bromoethyl-1-methylpyrrolidinium). Surprisingly, compound **2** displayed a reversible phase transition behavior at around 357 K, on the contrary, compound **1** showed no intention. Furthermore, although both **1** and **2** exhibited blue-white emission under UV light, it is worth noting that **2** showed two emission peaks by introducing the Cd^{2+} ion. It can be speculated that the regulation of the inorganic framework is of first importance for the difference in phase transition behavior and optical properties within such two compounds. Consequently, we have successfully designed a novel multifunctional material that associates reversible dielectric phase transitions with outstanding photoluminescence properties, developing new chances for potential applications in integrated optoelectronic devices.

1 Experimental

1.1 Synthesis

All chemicals and reagents are analytically pure and can be used without further purification. To synthesize compound **1**, 400 mmol of *N*-methylpyrrolidine was dissolved in 100 mL of acetonitrile, and then 400 mmol of 1,2-dibromoethane was added dropwise. The mixed solution was stirred at 70 ℃ for 48 h. The reacted mixture was distilled under reduced pressure and washed three times with ethyl acetate to obtain a brown solid, which was the product.

Compound **1** and $CdBr_2 \cdot 4H_2O$ were dissolved in

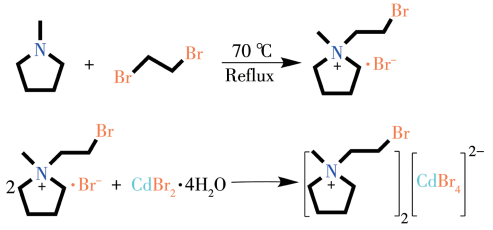

Scheme 1 Synthesis of compounds **1** and **2**

the mixed solution of water, methanol, and acetonitrile (1∶1∶1, *V*/*V*). The off-white crystals of compound **2** were obtained by slow evaporation of the mixed solution. The phase purity of the crystal was verified by powder X-ray diffraction (PXRD) and IR analysis (Fig. S1 and S2, Supporting information).

1.2 Physical measurements

Differential scanning calorimetry (DSC), PXRD measurement, dielectric measurements, and photoluminescence spectroscopy measurements are illustrated in the Supporting information. Variable-temperature single-crystal X-ray diffraction data for compounds **1** and **2** were collected using a Rigaku Syn007 diffractometer with Mo *Kα* (*λ*=0.071 073 nm) radiation in the *ω* scan mode.

2 Results and discussion

2.1 Thermal properties of 1 and 2

Thermal analysis is an effective means to detect temperature-induced phase transitions. The crystalline powders of both compounds were measured by DSC to confirm the reversible phase transition in the heating/cooling circle. As shown in Fig.1a, no apparent thermal anomaly was observed in compound **1**. After the smaller anion Br^- was replaced by the larger anion group $[CdBr_4]^{2-}$, a pair of endothermic and exothermic peaks appeared at 357.8 K/336.5 K in the heating/cooling cycle, indicating a reversible change (Fig.1b). The comparison of Fig.1a and 1b shows that the strategy of introducing Cd^{2+} to substitute larger metal framework anions for smaller individual inorganic anions to conduct phase transitions works well. As illustrated in Fig.1b, the wide hysteresis of 21.3 K and relative sharp peaks reveal that it is a first-order phase transition. Therefore, compound **2** undergoes a reversible first-order phase transition at around 357 K. According to the DSC curve, the ΔS for compound **2** was 34.44 J·mol·K^{-1}. Based on the Boltzmann equation, $\Delta S=R\ln N$, in which R is the gas constant and N is the number of possible orientations of the disordered system, the calculated N value of **2** was significantly greater than that of **1**, revealing the order-disorder characteristics of the phase transition.

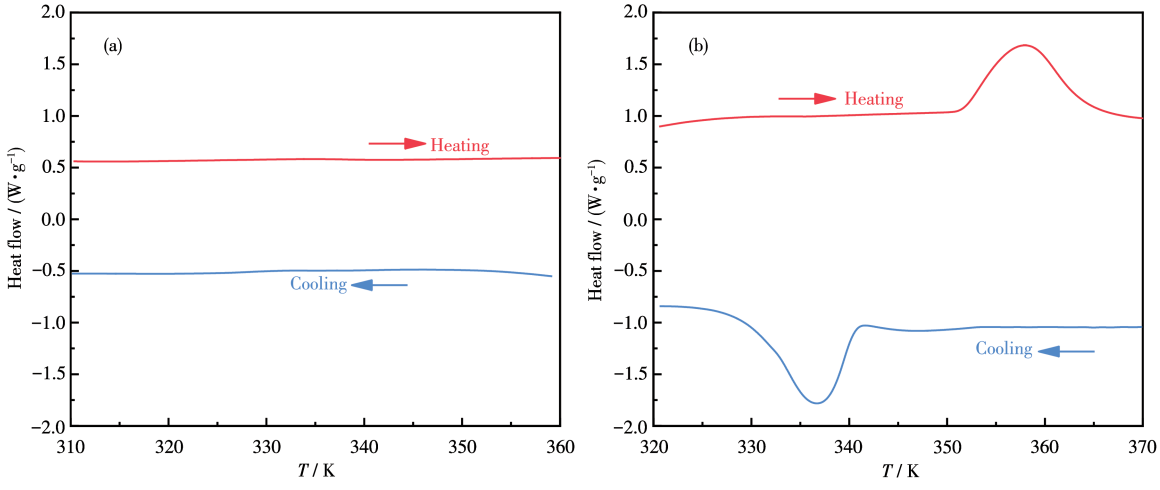

Fig.1　DSC curves of compounds **1** (a) and **2** (b)

2.2 Crystal structure analysis of 1 and 2

The single-crystal structure of **1** was obtained by X-ray diffraction measurements. It crystallizes in the orthorhombic non-central space group $Pna2_1$ with a=1.280 29(16) nm, b=0.667 95(8) nm, c=1.190 9(2) nm, Z=4, and V=1.018 4(2) nm^3 (Table S1). The asymmetric unit of **1** consists of a bempy cation and a Br^- anion (Fig.2a). All ions are in the ordered normal state.

For compound **2**, it crystallizes in the monoclinic centrosymmetric space group $P2_1/c$ at the low temperature (253 K), with a =1.552 21(7) nm, b=0.967 55(3) nm, c=1.726 45(7) nm, β=107.355(4)°, Z=4, and V=2.474 81(18) nm^3 (Table S2). The asymmetric unit of **2** is composed of two bempy cations and one monomeric

$[CdBr_4]^{2-}$ anion (Fig. 2b) that adopts a twisted tetrahedral structure with the Cd—Br bond lengths in the normal range of 0.256 50(8)-0.261 46(8) nm, and the Br—Cd—Br bond angles varying from 105.19(3)° to 111.99(3)° (Table S3). As illustrated in Fig. S3, compound **2** exhibits a 0D stacking structure at 253 K. As the temperature increased, the thermal motion of the molecules became more intense, bringing about the deterioration of the diffraction data, thus, we cannot obtain the specific high-temperature structure of compound **2**.

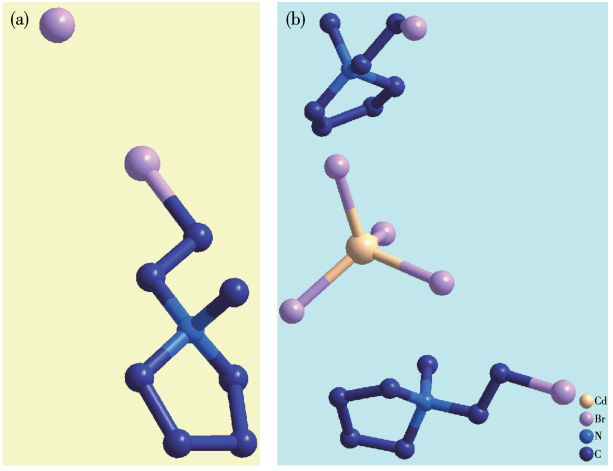

All hydrogen atoms are omitted for clarity

Fig.2 Asymmetric unit of compounds **1** (a) and **2** (b)

2.3 Variable-temperature PXRD analysis of 2

Variable-temperature PXRD experiments were fulfilled on compound **2** to further investigate more about the structural phase transition. As represented in Fig. 3, the difference in diffraction peaks was almost negligible below the phase transition point. However, the quantity and location of diffraction peaks changed more obviously when the temperature reached the phase transition point, especially in the 2θ degree range from 18° to 30°. The peak at 18.2° remained, but the peak at 19.1° disappeared. Simultaneously, diffraction peaks at 20.3°, 21.5°, and 22.7° were merged into two diffraction peaks at 21.2° and 22.3°. Besides, the diffraction peaks below 18° and over 30° have also shown diminutive distinction. Noticeable changes in diffraction peaks from low temperature to high temperature can be a piece of strong evidence to prove the occurrence of structural phase transition.

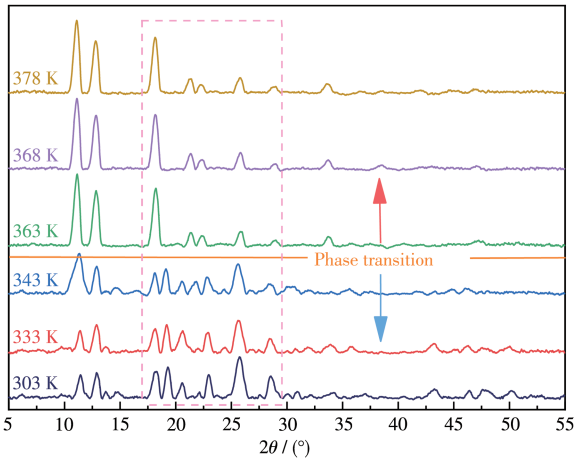

Fig.3 Variable-temperature PXRD patterns of **2**

2.4 Dielectric properties of 1 and 2

The temperature-dependent dielectric measurement is a reliable method to identify phase transitions as the dielectric constant, correlated with the nature of the phase transition, shows obvious abnormalities around the phase transition temperature. Compound **1** had no obvious dielectric anomalies in the heating-cooling curves (Fig. S4), conversely, compound **2** displayed a prominent step-like dielectric anomaly during the heating-cooling process, revealing a reversible phase transition (Fig.4a), which matched the DSC analysis well.

For compound **2**, a remarkable stepped dielectric anomaly was exhibited at 354 K after being heated. During the cooling cycle, the ε' of **2** decreased gradually to around 20 at high temperatures and then decreased rapidly at around 351 K, continuing to decrease slowly from 346 K, which manifested a clear slope in the curve. The abrupt change in the reversible dielectric constant in the heating and cooling curves confirms the existence of the reversible phase transition. To further detective the relationship between the dielectric constant and frequencies during the phase transition, the dielectric constant of **2** was measured at frequencies of 5, 10, 100 kHz, and 1 MHz. It illustrates that the phase transition temperature was independent of frequencies but the dielectric constant value decreased with the frequencies increasing (Fig.4b).

2.5 Photoluminescence properties of 1 and 2

The photoluminescence properties and intrinsic

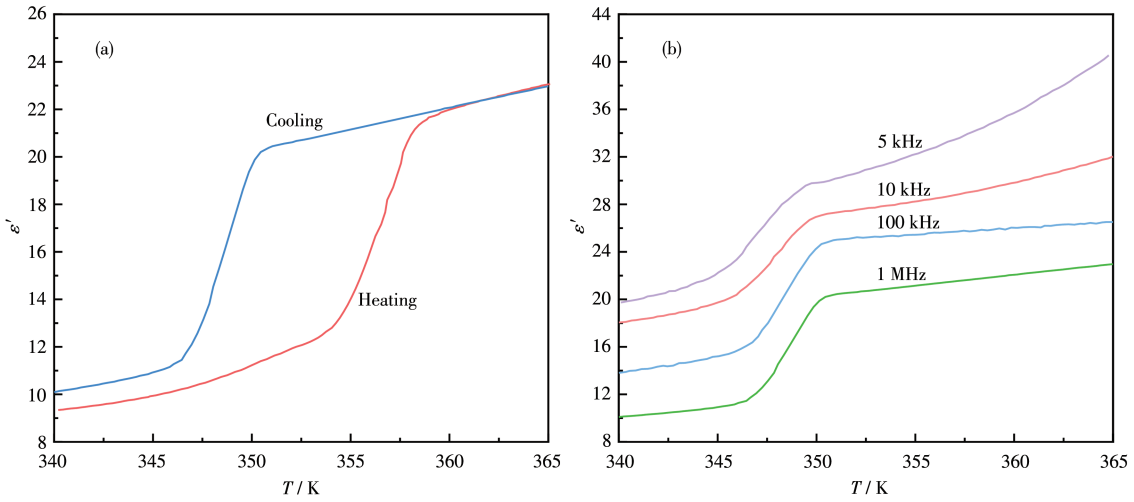

Fig.4　(a) Real part (ε') of the dielectric constant of **2** at 1 MHz in the heating and cooling curves; (b) Real part (ε') of the dielectric constant of **2** at 5, 10, 100 kHz, and 1 MHz in the cooling curves

mechanisms of compounds **1** and **2** were investigated at room temperature. The excitation spectra with a peak of around 300 nm for both compounds are shown in Fig. S5. The emission spectra of compounds **1** and **2** were obtained at the excitation wavelength of 307 nm (Fig.5a and 5b). It can be seen that **1** exhibited an emission maximum at 538 nm with a Stokes shift of 231 nm. For compound **2**, in addition to an emission peak at 547 nm, another emission peak appeared at 750 nm, which may be caused by $[CdBr_4]^{2-}$ anion. Both compounds exhibited broadband emissions that are attributed to blue-white light. The CIE chromaticity coordinates of the light emission were calculated as (0.271 1, 0.406 2) for **1** and (0.280 0, 0.417 9) for **2**, respectively (Fig.6a). The images in Fig. 6b and 6c represent the luminescence of **1** and **2** under UV irradiation, respectively, both of which show blue-white light emission. Compound **1** emitted very weak fluorescence under UV light, which may be caused by intermolecular interactions, while the fluorescence of compound **2** was slightly stronger, but not enough to be visible under natural light.

Structure determines properties. To explore the essential reasons for photoluminescence, the structural compositions of compounds **1** and **2** were determined. Compared with the emission spectra of **1** and **2**, at the same excitation wavelength, the emission peaks at around 540 nm were roughly the same location, but with different intensities. The emission peak of **2** was weaker than that of **1**. It is speculated that the photolu-

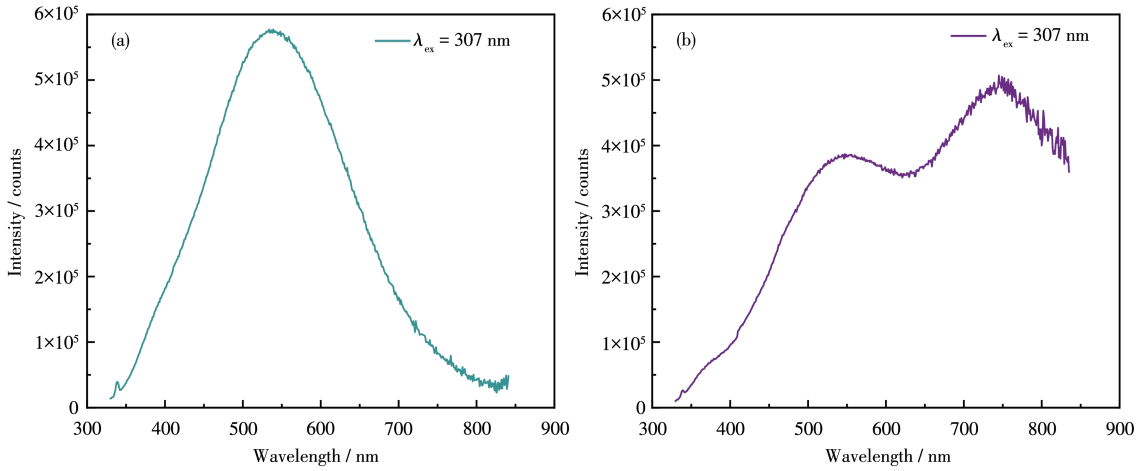

Fig.5　Emission spectra of compounds **1** (a) and **2** (b)

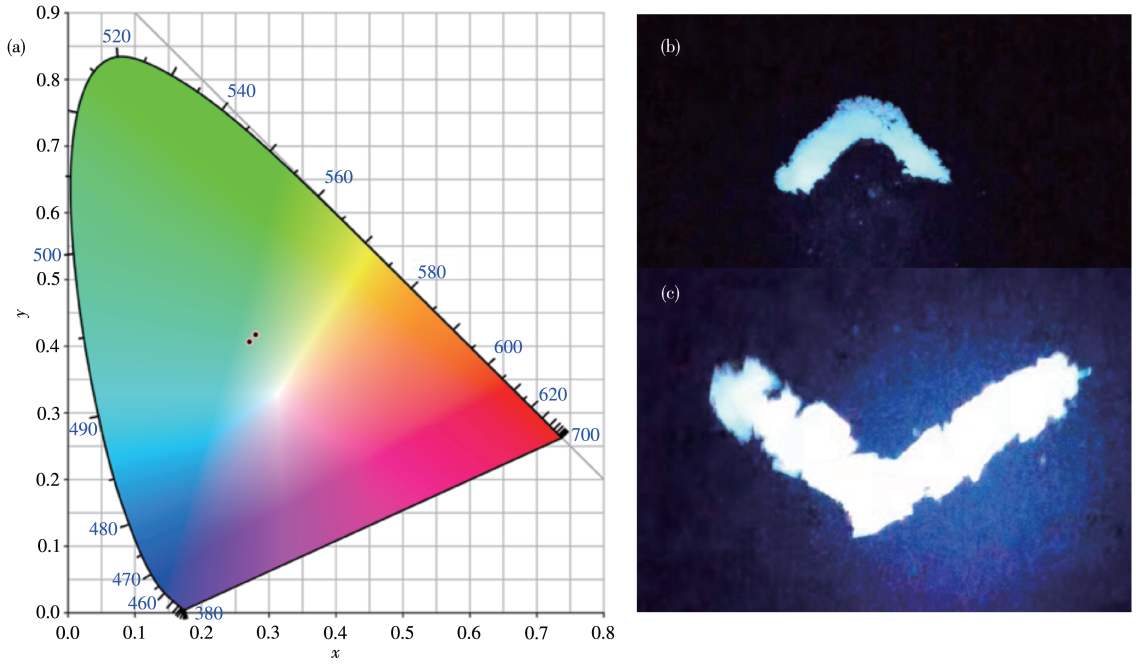

Fig.6 (a) CIE chromaticity coordinates of **1** (left) and **2** (right); Photographs of powder of (b) **1** and crystals of (c) **2** under UV light irradiation

minescence properties at around 540 nm are mainly derived from the organic cation bempy^{+}. Theoretically, the position of the fluorescence peak is influenced by compound structures and has nothing to do with the excitation wavelength. When Cd^{2+} was introduced into the inorganic framework, the anions-cations interaction might reduce the photoluminescence intensity and produce a new emission peak at 750 nm. For **2**, the emission intensity at 750 nm was significantly stronger than that at 547 nm. Moreover, the broadband blue-white light emission is ascribed as a combination of free exciton emission and self-trapped exciton emission[48]. The enlargement of the anion leads to a change in the emission peaks. Therefore, it is an effective strategy to change the position of the emission peaks through the regulation of the inorganic framework to obtain desired fluorescence properties. Regrettably, the disadvantage is that the quantum yields of **1** and **2** were not higher enough, and future research needs to focus on improving the quantum yield.

3 Conclusions

In summary, we have successfully prepared two crystalline compounds, in which the organic-inorganic hybrid halide $(bempy)_2CdBr_4$ (**2**) showed a reversible phase transition and efficient blue-white emission by introducing Cd^{2+}. In addition, the mechanism of its photoluminescence behavior may be originated from the synergistic effect of organic and inorganic components, and the intrinsic factor of broadband blue-white light emission probably benefits from the combination of free exciton emission and self-trapped exciton emission. Our work provides a design option for exploring multifunctional materials with more remarkable reversible phase transitions and tunable luminescence properties.

Supporting information is available at http://www.wjhxxb.cn

References:

[1]Zeng Y, Hu C L, Xu W J, Zeng T W, Zhu Z X, Chen X X, Liu D X, Chen Y J, Zhang Y B, Zhang W X, Chen X M. An Exceptional Thermally Induced Four-State Nonlinear Optical Switch Arising from Stepwise Molecular Dynamic Changes in a New Hybrid Salt. *Angew. Chem. Int. Ed.*, **2022**,**61**(2):e202110082

[2]Li M F, Xu Y M, Han S G, Xu J L, Xie Z D, Liu Y, Xu Z Y, Hong M C, Luo J H, Sun Z H. Giant and Broadband Multiphoton Absorption Nonlinearities of a 2D Organometallic Perovskite Ferroelectric. *Adv. Mater.*, **2020**,**32**(36):2002972

[3]Gao Y F, Zhang T, Zhang W Y, Ye Q, Fu D W. Great Advance in High T_c for Hybrid Photoelectric-Switch Bulk/Film Coupled with Dielectric and Blue-White Light. *J. Mater. Chem. C*, **2019**,**7**(32):9840-9849

[4]Zhang H Y, Jiang H H, Zhang Y, Zhang N, Xiong R G. Ferroelectric Lithography in Single-Component Organic Enantiomorphic Ferroelectrics. *Angew. Chem. Int. Ed.*, **2022**,**61**(22):e202200135

[5]Gao J X, Zhang W Y, Wu Z G, Zheng Y X, Fu D W. Enantiomorphic Perovskite Ferroelectrics with Circularly Polarized Luminescence. *J. Am. Chem. Soc.*, **2020**,**142**(10):4756-4761

[6]Zhou C K, Lin H R, Tian Y, Yuan Z, Clark R, Chen B H, van de Burgt L J, Wang J C, Zhou Y, Hanson K, Meisner Q J, Neu J, Besara T, Siegrist T, Lambers E, Djurovich P, Ma B W. Luminescent Zero-Dimensional Organic Metal Halide Hybrids with Near-Unity Quantum Efficiency. *Chem. Sci.*, **2018**,**9**(3):586-593

[7]Wang S S, Li L N, Sun Z H, Ji C M, Liu S J, Wu Z Y, Zhao S G, Zeb A, Hong M C, Luo J H. A Semi-conductive Organic-Inorganic Hybrid Emits Pure White Light with an Ultrahigh Color Rendering Index. *J. Mater. Chem. C*, **2017**,**5**(19):4731-4735

[8]Li M Z, Zhou J, Zhou G J, Molokeev M S, Zhao J, Morad V, Kovalenko M V, Xia Z G. Hybrid Metal Halides with Multiple Photoluminescence Centers. *Angew. Chem. Int. Ed.*, **2019**,**58**(51):18670-18675

[9]Su C Y, Lun M M, Chen Y D, Zhou Y C, Zhang Z X, Chen M, Huang P Z, Fu D W, Zhang Y. Hybrid Optical-Electrical Perovskite Can Be a Ferroelastic Semiconductor. *CCS Chem.*, **2022**,**4**(6):2009-2019

[10]Zhang T, Chu L L, Zhang Z X, Li J, Zhang W Y, Shi P P, Ye Q, Fu D W. Full-Temperature Covered Switching Material With Triple Optic-Dielectric States in a Lead-Free Hybrid Perovskite. *Sci China Mater.*, **2020**,**63**(11):2281-2288

[11]张齐, 张广威, 程军妍, 卢文欣, 王鹏. 基于羟乙氧基间苯二甲酸配体的Cd(Ⅱ)和Pb(Ⅱ)金属有机框架的合成、晶体结构及荧光性质. 无机化学学报, **2020**,**36**(11):2063-2070
ZHANG Q, ZHANG G W, CHENG J Y, LU W X, WANG P. Synthesis, Crystal Structure and Fluorescence Emission Properties of Cd(Ⅱ) and Pb (Ⅱ) MOFs Based on Hydroxyethoxy Isophthalate Acid. *Chinese J. Inorg. Chem.*, **2020**,**36**(11):2063-2070

[12]杨康, 谭育慧, 王宾, 周海涛, 李超, 杨昌善, 刘艺, 高继兴, 唐云志. 基于5-氨基-1*H*-1,2,4-三唑-3-羧酸的锌(Ⅱ)/锰(Ⅱ)配合物的合成、晶体结构及性质. 无机化学学报, **2019**,**35**(4):703-710
YANG K, TAN Y H, WANG B, ZHOU H T, LI C, YANG C S, LIU Y, GAO J X, TANG Y Z. Syntheses, Crystal Structures and Properties of Zn(Ⅱ), Mn(Ⅱ) Complexes Based on 5-Amino-1*H*-1,2,4-triazole-3-carboxylic Acid. *Chinese J. Inorg. Chem.*, **2019**,**35**(4):703-710

[13]喻敏, 宣芳, 刘光祥. 以4,4′-(1-咪唑基亚甲基)二苯甲酸为配体的锌配合物的合成、晶体结构和荧光性质. 无机化学学报, **2019**,**35**(1):133-140
YU M, XUAN F, LIU G X. Syntheses, Crystal Structures and Photoluminescent Properties of Two Zinc (Ⅱ) Coordination Polymers Derived from 4,4′-(1*H*-Imidazol-1-yl)methylene)dibenzoic Acid. *Chinese J. Inorg. Chem.*, **2019**,**35**(1):133-140

[14]Zhang Z X, Su C Y, Li J, Song X J, Fu D W, Zhang Y. Ferroelastic Hybrid Bismuth Bromides with Dual Dielectric Switches. *Chem. Mater.*, **2021**,**33**(14):5790-5799

[15]Zhang H Y, Chen X G, Zhang Z X, Song X J, Zhang T, Pan Q, Zhang Y, Xiong R G. Methylphosphonium Tin Bromide: A 3D Perovskite Molecular Ferroelectric Semiconductor. *Adv. Mater.*, **2020**, **32**(47): 2005213

[16]Yuan W, Zeng Y, Tan Y Y, Zhou J H, Xu W J, Zhang W X, Chen X M. A New Ferroelastic Hybrid Material with a Large Spontaneous Strain: $(Me_3NOH)_2[ZnCl_4]$. *Chem. Commun.*, **2019**,**55**(61):8983-8986

[17]徐慧婷, 刘洋, 秦刘磊, 齐欢欢, 刘尊齐. 1,4-二氮杂二环[2.2.2]辛烷-氰基合钴(Ⅲ)三维框架氢键型晶体的合成、相变及介电性质. 无机化学学报, **2021**,**37**(11):1950-1960
XU H T, LIU Y, QIN L L, QI H H, LIU Z Q. Synthesis, Phase Transition and Dielectric Properties of 1,4-Diazabicyclo[2.2.2]octane-Cyanide Cobalt (Ⅲ) Three-Dimensional Framework Hydrogen-Bonding Crystal. *Chinese J. Inorg. Chem.*, **2021**,**37**(11):1950-1960

[18]郑晓媛, 刘洋, 秦刘磊, 俞非凡, 朱春立, 刘尊齐. 氰基合钴(Ⅲ)氢键型笼状超分子晶体的合成、结构及介电性质. 无机化学学报, **2019**,**35**(2):277-284
ZHENG X Y, LIU Y, QIN L L, YU F F, ZHU C L, LIU Z Q. Synthesis, Structure and Dielectric Properties of Cyanide Cobalt(Ⅲ) Hydrogen-Bonding Cage-like Supramolecular Crystal. *Chinese J. Inorg. Chem.*, **2019**,**35**(2):277-284

[19]张子钰, 秦刘磊, 刘洋, 李辉, 胡宏志, 刘尊齐. 钼基吡啶类有机-无机杂化晶体材料的合成、可逆相变及介电性质. 无机化学学报, **2021**,**37**(2):305-315
ZHANG Z Y, QIN L L, LIU Y, LI H, HU H Z, LIU Z Q. Synthesis, Reversible Phase Transition and Dielectric Properties of Molybdenum-Based Pyridines Organic-Inorganic Hybrid Crystalline Materials. *Chinese J. Inorg. Chem.*, **2021**,**37**(2):305-315

[20]Chen X G, Song X J, Zhang Z X, Li P F, Ge J Z, Tang Y Y, Gao J X, Zhang W Y, Fu D W, You Y M, Xiong R G. Two-Dimensional Layered Perovskite Ferroelectric with Giant Piezoelectric Voltage Coefficient. *J. Am. Chem. Soc.*, **2020**,**142**(2):1077-1082

[21]Wu Y X, Wang C F, Li H H, Jiang F, Shi C, Ye H Y, Zhang Y. Highly Efficient and Uncommon Photoluminescence Behavior Combined with Multiple Dielectric Response in Manganese(Ⅱ) Based Hybrid Phase Transition Compounds. *Eur. J. Inorg. Chem.*, **2020**(4): 394-399

[22]Luo Y Y, Zhang Z X, Su C Y, Zhang W Y, Shi P P, Ye Q, Fu D W. Tunable Optoelectronic Response Multifunctional Materials: Exploring Switching and Photoluminescence Integrated in Flexible Thin Films/Crystals. *J. Mater. Chem. C*, **2020**,**8**(21):7089-7095

[23]Liu J Y, Ye S Y, Wan M, Wang Y N, Tong L, Chen L Z. A Novel Organic-Inorganic Hybrid Phase Transition Compound Based on 4-Ethylmorpholine with Switchable Dielectric and Luminescent Properties. *New J. Chem.*, **2022**,**46**(3):1054-1059

[24]Su C Y, Yao Y F, Zhang Z X, Wang Y, Chen M, Huang P Z, Zhang Y, Qiao W C, Fu D W. The Construction of a Two-Dimensional Organic-Inorganic Hybrid Double Perovskite Ferroelastic with a High T_c and Narrow Band Gap. *Chem. Sci.*, **2022**,**13**(17):4794-4800

[25]Zhang T, Ding K, Li J Y, Du G W, Chu L L, Zhang Y, Fu D W. Hydrogen-Bonded Engineering Enhancing Phase Transition Temperature in Molecular Perovskite Ferroelastic. *Chin. J. Chem.*, **2022**,**40**(3):1559-1565

[26]Zhang Y, Liao W Q, Fu D W, Ye H Y, Chen Z N, Xiong R G. Highly Efficient Red-Light Emission in an Organic-Inorganic Hybrid Ferroelectric: (Pyrrolidinium)$MnCl_3$. *J. Am. Chem. Soc.*, **2015**, **137**(15):4928-4931

[27]Ai Y, Chen X G, Shi P P, Tang Y Y, Li P F, Liao W Q, Xiong R G. Fluorine Substitution Induced High T_c of Enantiomeric Perovskite Ferroelectrics: (*R*)- and (*S*)-3-(Fluoropyrrolidinium)$MnCl_3$. *J. Am. Chem. Soc.*, **2019**,**141**(10):4474-4479

[28]Ye H Y, Zhou Q H, Niu X H, Liao W Q, Fu D W, Zhang Y, You Y M, Wang J L, Chen Z N, Xiong R G. High-Temperature Ferroelectricity and Photoluminescence in a Hybrid Organic-Inorganic Compound: (3-Pyrrolinium)$MnCl_3$. *J. Am. Chem. Soc.*, **2015**, **137**(40):13148-13154

[29]程赛楠, 丁坤, 宋泷藤, 张铁, 张志旭, 张毅, 付大伟. 1,4-二氮杂二环[2.2.2]辛烷衍生物的卤代作用有效诱导介电相变. 无机化学学报, **2021**,**37**(6):961-967
CHENG S N, DING K, SONG S T, ZHANG T, ZHANG Z X, ZHANG Y, FU D W. Dielectric Phase Transition Induced by Halogen Substitution Based on 1, 4-Diazabicyclo[2.2.2]octane-Derivatives. *Chinese J. Inorg. Chem.*, **2021**,**37**(6):961-967

[30]Xie Y F, Ai Y, Zeng Y L, He W H, Huang X Q, Fu D W, Gao J X, Chen X G, Tang Y Y. The Soft Molecular Polycrystalline Ferroelectric Realized by the Fluorination Effect. *J. Am. Chem. Soc.*, **2020**,**142**(28):12486-12492

[31]Wu Z Y, Zhang W C, Ye H, Yao Y P, Liu X T, Li L N, Ji C M, Luo J H. Bromine-Substitution-Induced High-T_c Two-Dimensional Bilayered Perovskite Photoferroelectric. *J. Am. Chem. Soc.*, **2021**,**143**(20):7593-7598

[32]Jiao S L, Yang Z, Jiao P J, Wu Y Y, Tang Z, Li D, Gao Z R, Sun X F, Cai H L, Wu X S. An Organic-Inorganic Hybrid Pyrrolidinium Ferroelectric Based on Solvent Selective Effect. *Inorg. Chem.*, **2021**, **60**(22):17212-1718

[33]Zhang H Y, Zhang Z X, Song X J, Chen X G, Xiong R G. Two-Dimensional Hybrid Perovskite Ferroelectric Induced by Perfluorinated Substitution. *J. Am. Chem. Soc.*, **2020**,**142**(47):20208-20215

[34]Tang Y Y, Xie Y F, Ai Y, Liao W Q, Li P F, Nakamura T, Xiong R G. Organic Ferroelectric Vortex-Antivortex Domain Structure. *J. Am. Chem. Soc.*, **2020**,**142**(52):21932-21937

[35]Chen Y Y, Gao C H, Yang T, Li W J, Xu H J, Sun Z H. Research Advances of Ferroelectric Semiconductors of 2D Hybrid Perovskites toward Photoelectronic Applications. *Chin. J. Struct. Chem.*, **2022**,**41**(4):1-11

[36]Liao W Q, Zeng Y L, Tang Y Y, Peng H, Liu J C, Xiong R G. Multichannel Control of Multiferroicity in Single-Component Homochiral Organic Crystals. *J. Am. Chem. Soc.*, **2021**,**143**(51):21685-21693

[37]Fu D W, Gao J X, He W H, Huang X Q, Liu Y H, Ai Y. High-T_c Enantiomeric Ferroelectrics Based on Homochiral Dabco Derivatives (Dabco=1,4-Diazabicyclo[2.2.2]octane). *Angew. Chem. Int. Ed.*, **2020**,**59**(40):17477-17481

[38]Wei Z H, Jiang Z T, Zhang X X, Li M L, Tang Y Y, Chen X G, Cai H, Xiong R G. Rational Design of Ceramic-like Molecular Ferroelectric by Quasi-spherical Theory. *J. Am. Chem. Soc.*, **2020**,**142**(4):1995-2000

[39]Xiong R G, Lu S Q, Zhang Z X, Cheng H, Li P F, Liao W Q. A Chiral Thermochromic Ferroelastic with Seven Physical Channel Switches. *Angew. Chem. Int. Ed.*, **2020**,**59**(24):9574-9578

[40]Nie Y, Zhang Z X, Shi P P, Zhang W Y, Ye Q, Fu D W. Flexible Thin Film and Bulk Switchable Relaxor Coexisting Most Optimal 473 nm Blue Light without Blue-Light Hazard/Visual Injury. *J. Phys. Chem. C*, **2019**,**123**(46):28385-28391

[41]Zhou J, Li M Z, Ning L X, Zhang R L, Molokeev M S, Zhao J, Yang S Q, Han K L, Xia Z G. Broad-Band Emission in a Zero-Dimensional Hybrid Organic [$PbBr_6$] Trimer with Intrinsic Vacancies. *J. Phys. Chem. Lett.*, **2019**,**10**(6):1337-1341

[42]Ji C M, Wang P, Wu Z Y, Sun Z H, Li L N, Zhang J, Hu W D, Hong M C, Luo J H. Inch-Size Single Crystal of a Lead-Free Organic-Inorganic Hybrid Perovskite for High-Performance Photodetector. *Adv. Funct. Mater.*, **2018**,**28**(14):1705467

[43]苏琼, 赵青, 安晓欣, 王彦斌, 李肖妍, 董文魁. 铜(Ⅱ)和镍(Ⅱ)Salamo型配合物的合成、晶体结构、Hirshfeld表面分析、热稳定和荧光性质. 无机化学学报, **2019**,**35**(3):524-536
SU Q, ZHAO Q, AN X X, WANG Y B, LI X Y, DONG W K. Syntheses, Crystal Structures, Hirshfeld Surface Analyses, Thermal and Fluorescent Properties of Cu(Ⅱ) and Ni(Ⅱ) Salamo-Type Complexes. *Chinese J. Inorg. Chem.*, **2019**,**35**(3):524-536

[44]Rok M, Zarychta B, Janicki R, Witwicki M, Bienko A, Bator G. Dielectric-Optical Switches: Photoluminescent, EPR, and Magnetic Studies on Organic-Inorganic Hybrid (azetidinium)$_2MnBr_4$. *Inorg. Chem.*, **2022**,**61**(14):5626-5636

[45]Sun X F, Li P F, Liao W Q, Wang Z X, Gao J X, Ye H Y, Zhang Y. Notable Broad Dielectric Relaxation and Highly Efficient Red Photoluminescence in a Perovskite-Type Compound: (*N*-Methylpyrrolidinium)$MnCl_3$. *Inorg. Chem.*, **2017**,**56**(20):12193-12198

[46]Zhang Z X, Su C Y, Gao J X, Zhang T, Fu D W. Mechanochemistry Enables Optical-Electrical Multifunctional Response and Tunability in Two-Dimensional Hybrid Perovskites. *Sci. China Mater.*, **2021**,**64**(3):706-716

[47]Yangui A, Pillet S, Bendeif E E, Lusson A, Triki S, Abid Y, Boukheddaden K. Broadband Emission in a New Two-Dimensional Cd-Based Hybrid Perovskite. *ACS Photonics*, **2018**,**5**(4):1599-1611

[48]Qi Z K, Chen Y L, Guo Y, Yang X L, Zhang F Q, Zhou G J, Zhang X M. Broadband White-Light Emission in a One-Dimensional Organic-Inorganic Hybrid Cadmium Chloride with Face-Sharing $CdCl_6$ Octahedral Chains. *J. Mater. Chem. C*, **2021**,**9**(1):88-94